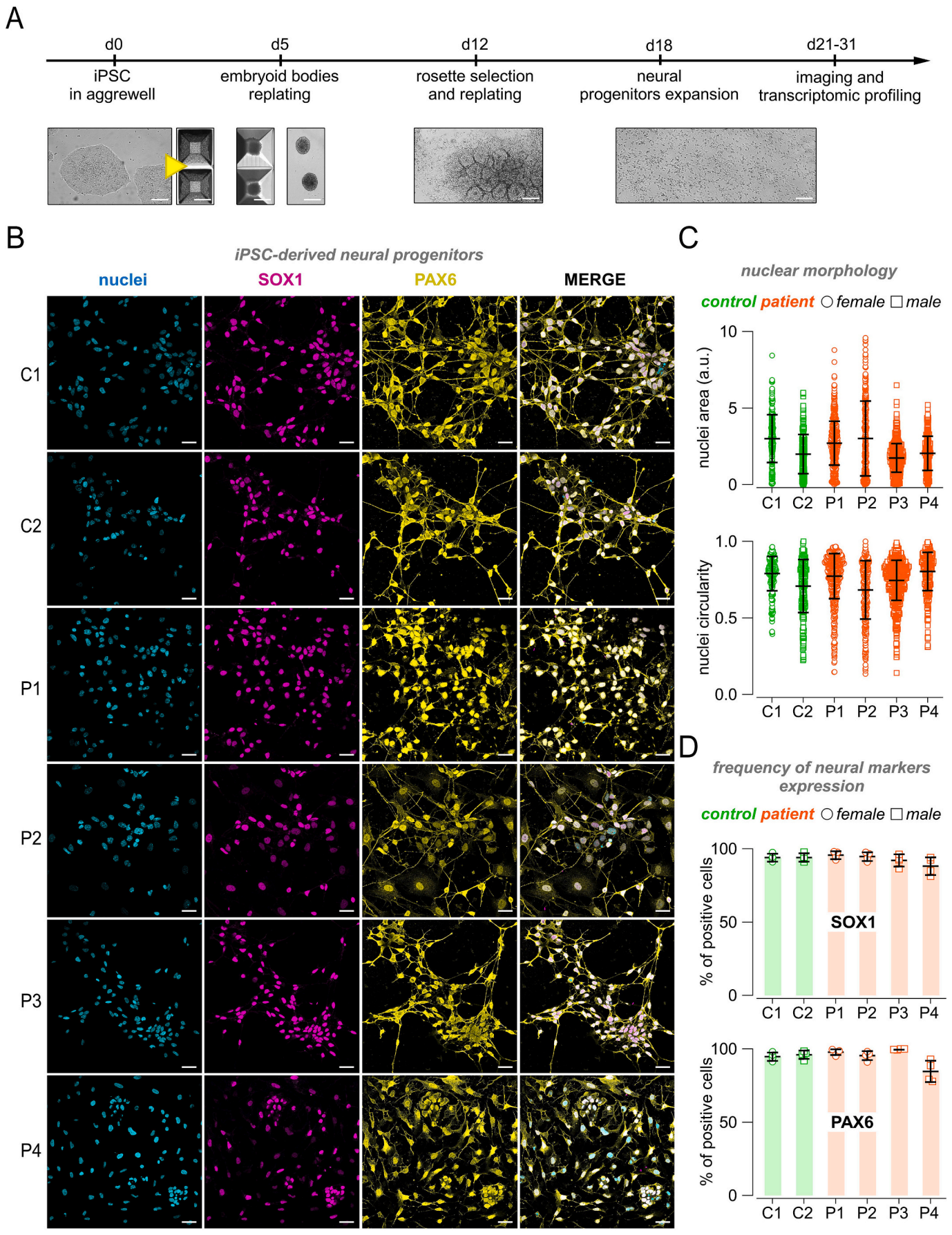

(caption on next page)

Fig. 3. Generation of iPSC-derived neural progenitors (NPC). (A) Schematic timeline of the multistep neural induction process, with representative brightfield images showing the progression from iPSCs to embryoid bodies, neural rosettes, and neural progenitor cells (NPCs). (B) Representative confocal images of iPSC-NPCs stained for SOX1 and PAX6, typical markers of early neural identity. Scale bar: 50 μm. (C) Dot plot graphs showing quantification of nuclear morphology (size and shape) in NPCs. At least 200 cells were analyzed for each line. (D) Quantitative analysis of the percentage of cells expressing neural markers, based on high-content imaging of samples as shown in panel B. Bar graphs represent mean ± S.D.; individual biological replicates are shown as dots ($n = 4$). Statistical analysis was performed by grouping data by condition (C1 and C2 as controls vs. P1-P4 as patient-derived lines). No statistically significant differences were detected by linear mixed models.

C). Immunofluorescence analysis demonstrated that patient-derived iPSC lines robustly expressed canonical undifferentiated state markers (OCT4, SSEA4, SOX2, and TRA-1-60), at levels comparable to those of previously established control lines, with more than 90 % of cells expressing each marker (Fig. 1D-E).

3.2. MWS iPSCs retain pluripotency and can differentiate into all three germ layers

We next evaluated the differentiation potential of MWS iPSC lines. Upon in vitro differentiation, both control and patient-derived lines were capable of generating cells expressing markers of the three germ layers: PAX6 and β3-tubulin for ectoderm, TBXT and TBX6 for mesoderm, and SOX17 and FOXA2 for endoderm (Fig. 2A). Quantitative analysis confirmed similarly high levels of lineage-specific marker expression across lines (Fig. 2B), supporting that MWS iPSCs retain full pluripotency.

3.3. Efficient generation of neural progenitor cells from MWS iPSCs

To model early neural development, iPSCs were differentiated into neural progenitor cells (NPCs) following a standard dual-SMAD inhibition protocol involving the sequential generation of embryoid bodies, neural rosettes, and NPCs (Fig. 3A). Immunostaining confirmed expression of early neural markers SOX1 and PAX6 in both control and MWS-derived NPCs (Fig. 3B). Morphometric analysis revealed no significant differences in nuclear shape or size (Fig. 3C), and the proportion of SOX1/PAX6-positive cells was comparable across lines (Fig. 3D), indicating efficient and consistent neural induction.

3.4. Transcriptional profiling reveals altered neural identity in MWS NPCs

RNA-seq analysis of iPSC-derived NPCs uncovered significant transcriptional alterations in MWS lines compared to controls. To explore potential changes in cell identity, we focused on panels of genes representing established markers of different brain cell lineages (Ianevski et al., 2022) (Fig. 4). Both control and MWS NPCs showed lack of expression of pluripotency genes, including *NANOG*, *TDGF1*, *FGF4*, and *DPPA2*, confirming exit from the undifferentiated state (Fig. 4A). Lineage-specific markers revealed more subtle differences. Early neuroepithelial genes such as *NOTCH1*, *HES1*, *SOX1*, and *SOX2* were expressed at comparable levels between groups, whereas radial glial markers *NES*, *PAX6*, and *SLC1A3* were significantly reduced in MWS NPCs (Fig. 4A, B). Within the glial lineage markers, MWS NPCs showed a trend toward reduced expression of the Schwann cell precursor marker *GAP43* and increased expression of the oligodendrocyte precursor cell (OPC) marker *CSPG4*, although these differences did not reach statistical significance (Fig. 4C, D). As expected at this developmental stage, markers of mature glial cells (including Schwann cells, oligodendrocytes, and astrocytes) remained largely silent across all samples, except for *NCAM1*, which showed relatively high expression (Fig. 4C). Early and mature neuronal markers were also examined. The neurogenic regulators *ASCL1* and *DCX* were expressed at high levels, with slight reductions observed in three out of the four patient lines (Fig. 4E, F). Markers of mature neurons, such as *SYP* and *SLC16A7*, were expressed at very low levels, while GABAergic neuronal markers including *SLC32A1*, *GAD1*, and *GAD2* showed medium-low expression in controls and variable, often reduced, expression in MWS lines (Fig. 4E, F). When comparing all control versus all MWS NPCs as groups, these differences did not reach statistical significance (Fig. 4E, F).

Altogether, these findings indicate that *ZEB2* variants alter transcriptional programs governing radial glial development and may subtly influence neuronal subtype specification, which could contribute to neurodevelopmental deficits in MWS.

3.5. Differential gene expression and pathway enrichment in MWS NPCs

To investigate global gene expression changes, we performed differential expression analysis between MWS and control iPSC-derived NPCs. We identified 43 significantly downregulated and 116 significantly upregulated genes in MWS cells compared to controls (Fig. 5A). The top 40 differentially expressed genes in each group are shown in Fig. 5B and C.

Notably, downregulated genes with known roles in neurogenesis included *CER1* (a cytokine essential for anterior neural induction), *PCP4* (a positive regulator of neuronal differentiation), *BEND6* (which promotes neuronal differentiation by repressing neural stem cell self-renewal), *SLCO1C1* (an organic anion transporter involved in GABAergic interneuron development), *SPARCL1* (involved in synapse formation), *CACNB2* (which encodes a beta subunit of voltage-gated calcium channels), and *DOC2B* (a calcium sensor critical for synaptic vesicle release) (Dai et al., 2013; Diez et al., 2021; Friedrich et al., 2008; Friedrich et al., 2008; Hou et al., 2013; Kucukdereli et al., 2011; Martins et al., 2022; Mayerl et al., 2022; Mouton-Liger et al., 2011). Additionally, some downregulated genes have been also implicated in neurodevelopmental disorders: *GABBR2* (developmental and epileptic encephalopathy), *CPNE6* (epilepsy and neuromuscular disease), *KCNN3* (Zimmermann-Laband syndrome-3), and *MCHR1* (linked to bipolar disorders) (Anazi et al., 2017; Bauer et al., 2019; Gripp et al., 2021; Mullins et al., 2021; Yoo et al., 2017).

Conversely, many upregulated genes in MWS NPCs were associated with extracellular matrix remodeling and non-neural lineage specification. Among the former, we found ECM structural genes (*COL1A1, COL1A2, COL5A1, COL12A1, COL13A1, COL26A1*), ECM-associated glycoproteins (*FBLN2, EMILIN1, EGFL6, NID2, HAPLN1*), ECM modulators (*MMP25, PCOLCE*), adhesion-related genes (*CD248, KIRREL2, ITGA5*, *ISLR, DSP, CLDN11*), and migration and matrix signaling genes (*EMCN*, *LAMC3*) (Theocharis et al., 2016). Regarding non-neural lineage specification, we found up-regulation of genes involved in vascular development, including *EMILIN1* and *PEAR1* (vascular stability and adhesion), *CASZ1*, *EDNRA*, *ADGRA2*, and *PLXDC1* (angiogenesis and vessel remodeling), *APLNR*, *ANGPT2*, and *ENG* (angiogenesis signaling) (Adamo et al., 2022; Akwii et al., 2019; Eubelen et al., 2018; Liu et al., 2023; Mughal and O'Rourke, 2018; Vandenbriele et al., 2015). Furthermore, upregulation of genes involved in skeletal development (e.g., *OGN*, *BGN*, *CREB3L1*, *ITM2A*, *KAZALD*, *MSX2*) and Wnt signaling regulators (e.g., *DKK2*, *FRZB*) was also observed, suggesting aberrant activation of non-neural developmental programs in MWS NPCs (Berendsen et al., 2014; Bodine and Komm, 2006; Hock et al., 2001; Keller et al., 2018; Lories et al., 2013).

Gene Ontology (GO) enrichment analyses based on DEGs revealed a substantially higher number of enriched pathways among upregulated genes. KEGG pathway analysis highlighted significant enrichment in pathways associated with protein digestion and absorption, PI3K-Akt signaling, Relaxin signaling, focal adhesion, and extracellular matrix

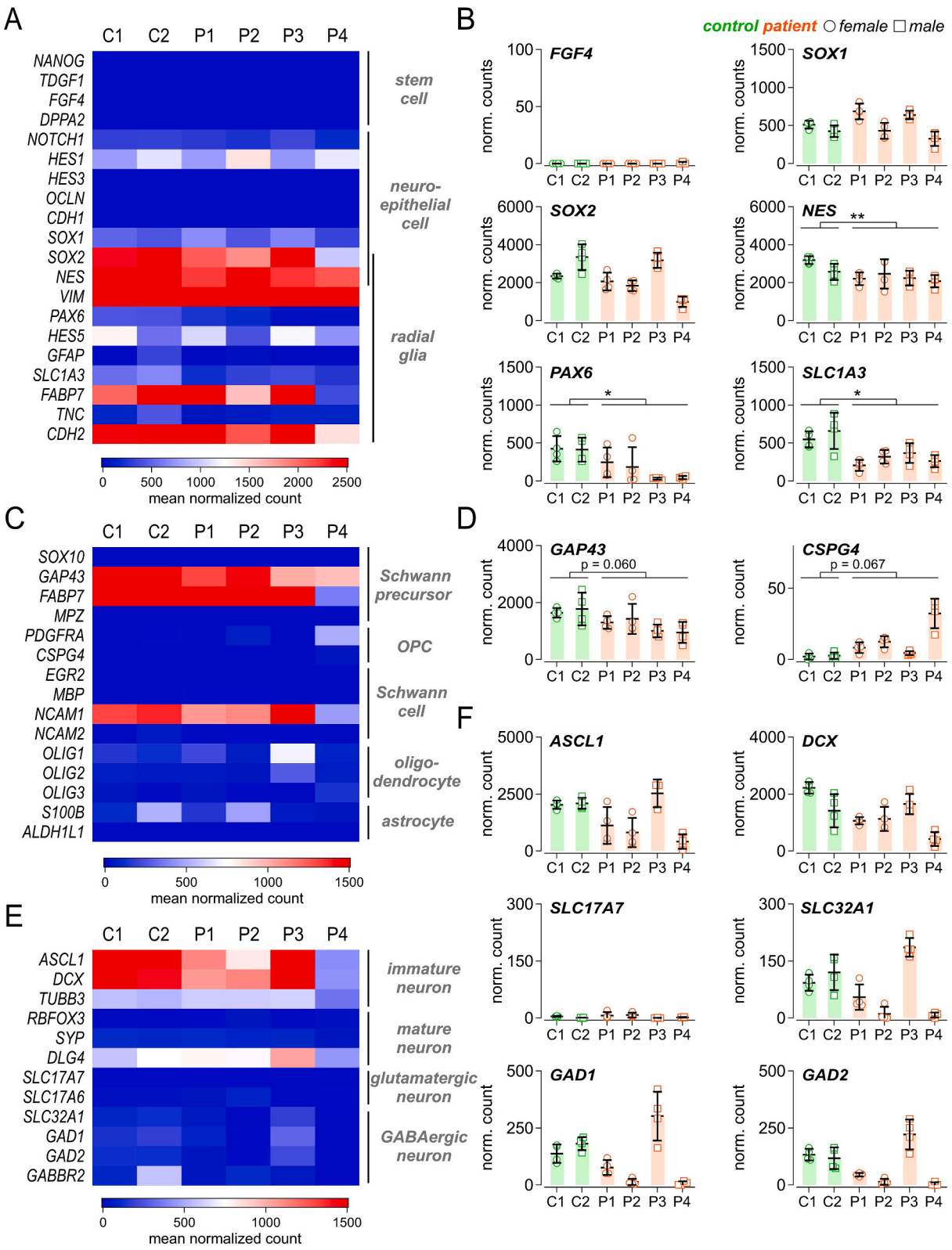

Fig. 4. Transcriptional profiling of MWS iPSC-derived NPCs. (A, C, E) Heatmaps showing mean normalized expression levels of genes associated with distinct neural cell identities and developmental states. (A) Markers of stem cells, neuroepithelial cells, and radial glia. (C) Markers of Schwann cell precursors, oligodendrocyte precursor cells (OPCs), Schwann cells, oligodendrocytes, and astrocytes. (E) Markers of immature neurons, mature neurons, glutamatergic neurons, and GABAergic neurons. (B, D, F) Quantitative plots of normalized expression levels for selected genes shown in the corresponding heatmaps. Bar graphs represent mean ± S.D.; individual biological replicates are shown as dots (n = 4). Statistical analysis was performed by grouping data by condition (C1 and C2 as controls vs. P1-P4 as patient-derived lines). *, $p < 0.05$; **, $p < 0.01$ determined by linear mixed models.

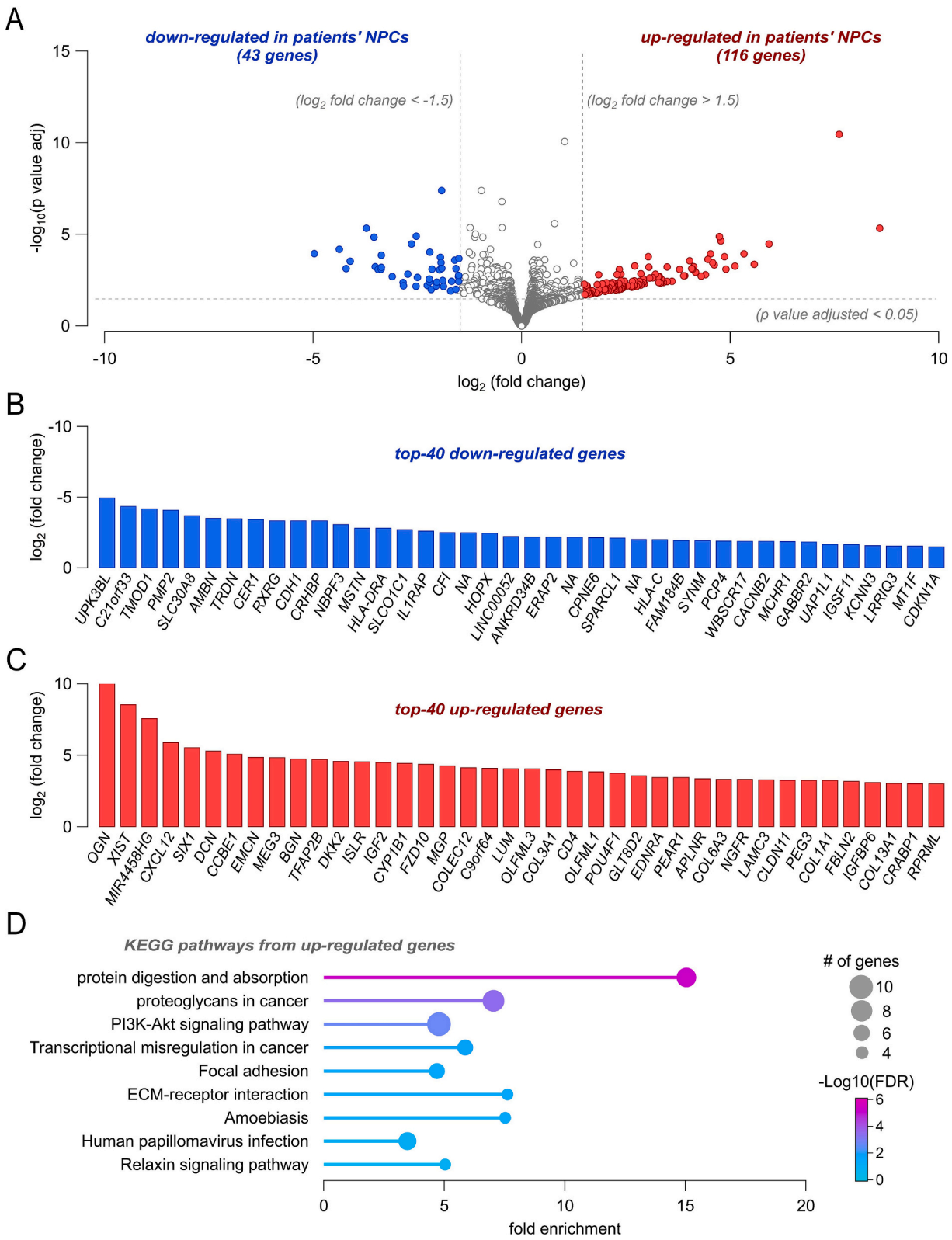

Fig. 5. Analysis of differentially expressed genes in MWS iPSC-derived NPCs. (A) Volcano plot showing differentially expressed genes (DEGs) between control and patient iPSC-derived NPCs from RNA-seq data. Genes with $\log_2$ fold change < -1.5 and adjusted $p < 0.05$ are shown in blue; those with $\log_2$ fold change >1.5 and adjusted $p < 0.05$ are shown in red; non-significant genes ($-1.5 < \log_2$ fold change <1.5 and/or adjusted $p > 0.05$) are shown in gray. (B, C) Bar plots of the top 40 significantly downregulated (B) and upregulated (C) genes in MWS NPCs compared to controls. (D) Gene Ontology enrichment analysis of up-regulated genes, highlighting KEGG pathways ranked by fold enrichment, false discovery rate (FDR), and number of differentially expressed genes per pathway. All analyses were performed using transcriptomic data from four preparations of iPSC-derived NPCs (n = 4). (For interpretation of the references to colour in this figure legend, the reader is referred to the web version of this article.)